Available online at www.sciencedirect.com
SCIENCE DIRECT
Polymer 47 (2006) 5012–5024
polymer
www.elsevier.com/locate/polymer

Batch foaming of poly(ε-caprolactone) using carbon dioxide: Impact of crystallization on cell nucleation as probed by ultrasonic measurements

Joël Reignier *, Jacques Tatibouët, Richard Gendron

Industrial Materials Institute, National Research Council Canada, 75 de Mortagne Boulevard, Boucherville, QC, Canada J4B 6Y4

Received 24 March 2006; received in revised form 16 May 2006; accepted 17 May 2006
Available online 6 June 2006

Abstract

The effect of crystallization on the foaming of poly(ε-caprolactone), a semi-crystalline biodegradable polymer, was studied using batch processing and CO_2 as the physical blowing agent (PBA). Previous work on the same system suggested that the formation of high cell population densities of small open cells was crystalline fraction dependent. In this work, ultrasonic sensors were used to investigate the effect of crystallization on the cell nucleation mechanism through the monitoring of ultrasonic velocity, attenuation and specific volume characteristics. Analysis of the ultrasonic data allowed to determine the crystallization temperature and thus determined the effect of crystallization on the pressure at which phase separation occurred (degassing pressure). Clearly, the presence of crystals leads to a 5–10-fold increase in the degassing pressure with respect to the amorphous system. In addition, it was shown that the talc content did not significantly influence the degassing pressure for a full amorphous system. However, talc particles can drastically affect the degassing conditions through their role of precursors for crystal formation. Different mechanisms are proposed as possible explanations for the enhancement of cell nucleation in such semi-crystalline polymer systems.

Keywords: Cell nucleation; Ultrasonic measurements; Crystallization

1. Introduction

Control of cell nucleation during foaming of polymer/PBA systems is a key factor for the morphology and the density of the resulting foams. Traditionally, this is generally achieved by addition of a small amount of inorganic filler (talc, TiO_2, $CaCO_3$,…). According to the classical heterogeneous nucleation theory, revisited by Colton and Suh [1] for amorphous thermoplastic systems, the energy barrier associated with the formation of a critical nucleus of PBA can be greatly reduced by the existence of an interface between the polymer/PBA mixture and a solid particle. However, while the underlying concept in that theory is that the PBA molecules must migrate toward the said interface, there is almost no data available to validate this hypothesis. This diffusion may also be questionable since the presence of polymer macromolecules already adsorbed on the surface of these solid particles, with strong interaction favored by high energetic particles, may restrain considerably the PBA nucleus formation at that specific location.

Several alternative mechanisms have been proposed to explain heterogeneous nucleation in filled polymers. Chen et al. [2] observed that gas absorption increases in the presence of fillers ($CaCO_3$, talc) and suggested that a certain amount of gas accumulates inside the micro-pores at the polymer-filler interface which thus helps to nucleate cells during the foaming process. However, this hypothesis of an enhanced dissolution was not validated using a much more accurate measurement device: Areerat et al. [3], using a magnetic suspension balance, determined the same solubility of carbon dioxide in polyethylene, whether the polymer was charged with titanium dioxide particles or not, which preclude then the existence of a gas-rich interface. Ramesh et al. [4] developed a new model for bubble nucleation in a PS matrix containing polybutadiene rubber dispersed particles, based on pre-existing microvoids at the rubber/polymer interface—these microvoids would result from the thermal processing history of the polymer—which then will favour bubble nucleation at the interface. In another approach, Tatibouët et al. [5], using an in-line ultrasonic

* Corresponding author. Tel.: +1 450 641 5201; fax: +1 450 641 5105.
E-mail address: joel.reignier@cnrc-nrc.gc.ca (J. Reignier).

0032-3861/$ - see front matter
doi:10.1016/j.polymer.2006.05.040

method, showed that the addition of a small amount of talc or TiO_2 during the foam extrusion of a PS/HCFC–142b system increases the degassing pressure, this latter defined as the pressure at which phase separation between PBA and polymer matrix occurred. These higher degassing pressures were also associated with enhanced cell density in the resulting foams. By considering free energy concepts, they suggested in a following study [6] that the concentration of PBA might not be uniform throughout the whole polymer matrix but may be higher in some domains close to, but not at the interface, of the nucleating agent particles, with the higher concentration areas responsible for the higher than expected degassing pressures. Unfortunately, this hypothesis on possible PBA gradient within the polymer matrix is quite difficult to verify. Despite these numerous papers on the influence of solid particles on cell nucleation of amorphous polymer matrix, it seems that a thorough understanding of the mechanisms controlling the heterogeneous nucleation in viscoelastic fluids is still in its pioneering stage.

Little work has been done on the influence of crystallinity on cell nucleation in a semicrystalline polymer/PBA system. Many papers report an improvement of cellular morphology with crystalline content, yielding smaller cell size and higher cell population density, compared to completely amorphous systems. This seems to indicate that crystallites result in higher cell nucleation densities in such a way a classical nucleating agent does [7,8]. Baldwin et al. [7] claimed that the crystallites can be considered as additive particles and thus increases heterogeneous nucleation contribution by decreasing the Gibbs free energy associated with the formation of stable PBA clusters at the amorphous/crystal interfaces. However, according to Doroudiani et al. [9] who studied the effect of crystallinity on the microcellular foam structure of semicrystalline polymers (HDPE, PB, PP and PET), the cold-water-quenched samples (less crystalline and smaller spherulite size) produced more uniform and finer cellular structures compared to the slow cooled samples (higher crystalline fraction and larger spherulite size), which exhibit only a few locally foamed areas due to the higher matrix stiffness.

Using a different approach, Handa et al. [10] pointed out that classical heterogeneous nucleation cannot be applied in the case of semi-crystalline polymers since the boundaries between amorphous and crystalline parts are not well defined. In addition, they also mentioned that the crystallized part has lower surface energy than the amorphous part, and this cannot trigger bubble nucleation at the surface of the crystallized parts. In that case, they explained the higher cell nucleation densities observed in syndiotatic polystyrene (sPS) for meso-sPS and α-sPS phases by the presence of microvoids (the amorphous part in meso and α forms were found to absorb about 60 wt% more CO_2 gas than the regular amorphous sPS when normalized with respect to 100% amorphous content) which could then be the preferred sites for gas nucleation. They associated these microvoids with the so-called rigid amorphous phase that bridges the amorphous phase and the crystalline phase. The existence of rigid amorphous phase in semi-crystalline polymer such as PET is now well recognized and is associated with the region where several lamellas are separated by very thin (2–4 nm) amorphous layers. Even if these regions possess additional free volume upon cooling, which may explain the observed higher solubility [11], it is hard to believe that they can participate to bubble nucleation and growth since they are constrained between crystallites. It is also of interest to point out the work done by Mizoguchi et al. [12] on the formation of micro-cavities in semicrystalline systems during the desorption of the CO_2 gas molecules. These authors illustrated that using PET samples, for which the plasticizing effect of absorption of CO_2 gas molecules is high enough to decrease the T_g and thus to induce crystallization at ambient temperature. They nicely showed that the density of the sample crystallized with dissolved CO_2 was smaller ($\cong 0.003$ g /cm^3) than that of a thermally crystallized sample having the same crystallinity level. This difference was attributed to the presence of crystallites that would hinder the relaxation of the structural volume when the polymer changes from the rubbery to the glassy state upon the release of the CO_2 molecules. Unfortunately, the nature of these microvoids, e.g. discrete locations or uniformly distributed in the free volume, remained unknown. This observation may also be applied to a semicrystalline polymer that is simply cooled from the rubber state to the glassy state with respect to a completely amorphous sample.

A previous work on the foaming of PCL in batch processing using carbon dioxide [13] has shown that the apparition of a finer cell structure at low foaming temperature was crystalline dependent. As shown in Fig. 1, PCL/talc/CO_2 systems with different talc concentrations (0.5–5 wt%) foamed at a temperature of 32 °C displayed a bimodal cell structure, which was explained by different levels of crystallinity. Accordingly, it was proposed that the coarse cell structure corresponds to highly amorphous regions whereas the finer open-cell structure was associated with more crystalline regions. The role of crystals as nucleating sites or promoters for bubble formation needs to be correctly addressed. The aim of the present work is to elucidate this interesting question. In order to avoid the possible issue of coalescence phenomena generally encountered in estimating of cell nucleation density on final foam products, we have chosen to study the effect of crystallization on cell nucleation using ultrasonic measurements. This novel technique has been found to be very efficient to monitor the crystallization phenomena [14] as well as to probe cell nucleation in foaming experiments through measurement of the degassing pressure [5,6]. In this paper, we carefully examine the nature of the changes in nucleation resulting from crystallization and propose an explanation for the possible mechanisms.

2. Experimental

2.1. Material

A commercial grade of poly(ε-caprolactone) (Tone P-787 from Dow Chemicals), with a number-average molecular weight of 80,000 g/mol corresponding to a melt flow index of 0.5 g/10 min, was used for the investigation. The nucleating agent was talc (Mistron Vapor-R from Luzenac Corporation) with a mean particle size of 2 μm and a specific surface of

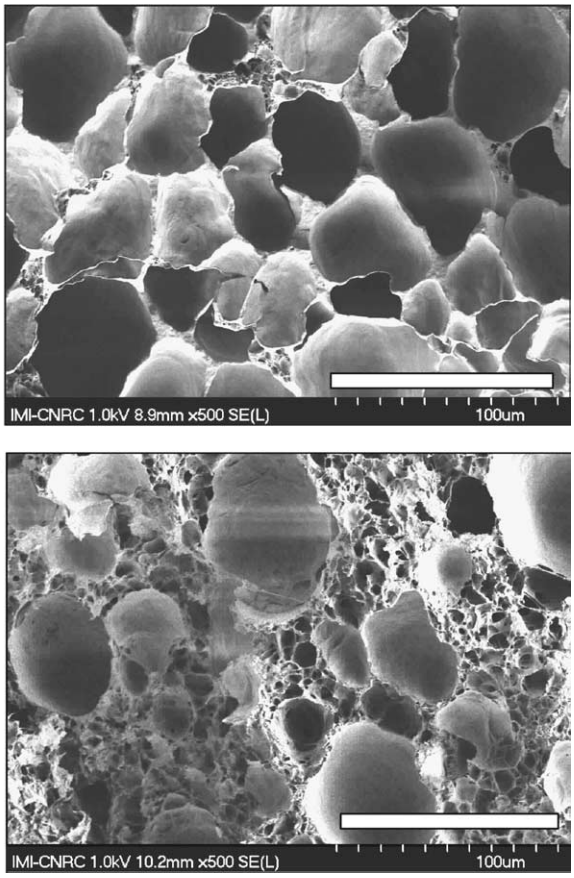

Fig. 1. SEM photomicrographs of PCL/talc/CO_2 samples with different talc concentrations: (a) 0.5 wt%; (b) 5 wt%. The samples were foamed at $T=32$ °C after slow cooling from the melt state. The samples were allowed to saturate for 2 h at a saturation pressure of about 6.5 MPa (940 psi) and a temperature of 70 °C. In both cases, the white bar denotes 100 μm. Clearly, increasing talc content increases the surface fraction of finer cell structure compared to the coarser one [13].

13.4 m^2/g. The concentration of talc in the material with nucleating agent was set to 5 wt%.

2.2. Solubility measurements

The CO_2-gas equilibrium absorption of PCL and PCL/5 wt% talc were investigated by a gravimetric method. Samples ($1\times 20\times 20$ mm^3) were obtained from compressed mold sheets and weighted prior their introduction in a pressure vessel. They were maintained for 2 days at constant CO_2 pressure ranging from 0.69 to 5.51 MPa and at a temperature close to 24 °C. Once the required saturation time was reached, the pressure was quickly released (in approximately 15 s), the sample removed and weighted as quickly as possible, as a function of time (i.e. typically within 1 min). These desorption experiments allowed us to estimate by extrapolation the concentration of CO_2 dissolved into the sample at the end of the sorption time [13].

2.3. Ultrasonic measurements

Samples were molded from pellets to obtain discs (32 mm diameter, 3 mm thick) under 20 MPa and at 120 °C using the static ultrasonic measurement apparatus, which is described in details elsewhere [15]. These discs were then placed in a pressure vessel filled with CO_2 and maintained at room temperature with the blowing agent pressure around 4.8 MPa during 2 days. Based on our previous work [13], this saturation time was found to be sufficient to ensure that equilibrium sorption was reached. After pressure release, the sample was quickly transferred to the ultrasonic measurement device where a pressure of 20 MPa was immediately applied to prevent undesired foaming or gas loss. The ultrasonic measurement system is gas tight and by reducing progressively the applied pressure ($dP/dt=-1$ MPa/min) one can induce phase separation and foaming at a given temperature without loss of blowing agent. During this operation, ultrasonic characteristics (attenuation and sound velocity) can be monitored as well as specific volume. The degassing pressure related to the onset of bubble nucleation was determined as the pressure corresponding to the abrupt attenuation rise [16]. More details will be given in the following sections. Increasing again the pressure allowed the gas to dissolve back in the material, and to return to the initial state after some minutes. Precise concentration of blowing agent was later determined by weighing the sample before and after final degassing outside the device in an oven under vacuum.

2.4. Foaming experiments

Batch foaming experiments were carried out by cooling down the PCL/CO_2 solution from the melt as reported in a previous study [13]. PCL/talc samples were placed in a pressure vessel and saturated for 3 h at 70 °C and a CO_2 pressure of around 6.2 MPa. Then the temperature was freely cooled down to the desire foaming temperature, set at 32 °C. Once the temperature was reached, the applied pressure was quickly decrease (in approximately 45 s) to a given controlled decompression level, denoted as P_{decomp}, for a period of time of roughly 5 min. The samples were then cooled down to ambient temperature in order to freeze in the morphology through crystallization, before completely releasing the pressure to atmospheric pressure. The samples were finally fractured in liquid nitrogen and characterized using a Hitachi scanning electron microscope.

3. Results and discussion

3.1. Characterization of unfoamed gas-swollen polymer samples

Prior to degassing pressure measurements, the samples were ultrasonically characterized at a constant pressure of $P=$ 10 MPa. This pressure was found to be high enough to prevent phase separation and bubble formation. Attenuation as well as sound velocity were measured during cooling from 110 to −80 °C at a cooling rate of 2 °C/min and these characteristics are reported on Fig. 2 for specimens with and without blowing agent. In a general manner, the results illustrate the

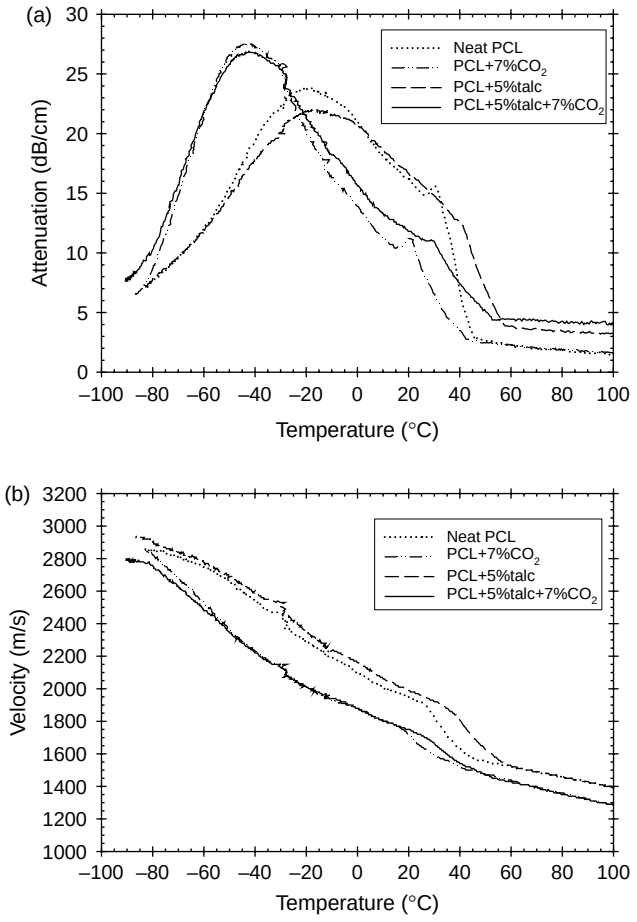

Fig. 2. Evolution of (a) sound attenuation and (b) velocity during cooling experiment (−2 °C/min) performed under a pressure of 10 MPa.

plasticization of the polymer material by CO_2 and the change in crystallization kinetics due to the blowing agent and the nucleating agent.

The abrupt increase in attenuation when the material is cooled from the melt in the temperature range from 40 to 60 °C is attributed to the crystallization and the growth of crystallites [14,17] and its onset can be used to determine the crystallization temperature. The presence of CO_2, which increases free volume and affects the mobility of the polymer chains, such as a plasticizer usually does, slightly decreases the crystallization temperature by roughly 5 °C on continuous cooling. Similar effect of CO_2-delayed crystallization have been reported in a previous work on PCL/CO_2 system [13] and for isotactic polypropylene [18] using High Pressure DSC. On the contrary, the effect of talc is more significant since talc increases this crystallization temperature by approximately 13 °C. Another interesting characteristic excerpted from the attenuation graph is given by the slope of the 'crystallization peak', which can be related to the number of crystallization nuclei and also to the crystallite growth rate. As our experiments are performed in non-isothermal way, the interpretation remains complex. However, for both cases without CO_2, the slopes as determined over the same temperature range, e.g. 40–45 °C, are the same, indicating that the crystallization process is not drastically modified by the talc, except for the early initiation of crystallization due to the presence of the particles. On the contrary, CO_2 slows the crystallization rate. Indeed, the concentration of CO_2 molecules, exclusively located in the amorphous phase, increases with increasing crystalline fraction, which means in other words that the concentration of CO_2 in the amorphous phase increases as the temperature decreases. Similar effects of CO_2 have been reported by Zhang et al. [18] on the crystallization kinetics of PP.

The relaxation peak observed at lower temperature is related to the α-relaxation of the amorphous phase. The increase of its amplitude with the presence of CO_2 indicates that addition of CO_2 leads to materials with reduced crystallinity, according to our previous results obtained on a high pressure DSC [13]. However, the addition of talc obviously does not affect the temperature associated with the α-relaxation and does not modify the final crystallinity. On the other side, the temperature shift of this relaxation peak from roughly −20 to −45 °C when 7 wt% of CO_2 is dissolved in the PCL illustrates well the strong plasticization of the material by the blowing agent. Comparison of the shift in the crystallization temperature due to the presence of talc indicates that talc-induced crystal nucleation is not modified by CO_2-induced PCL plasticization, since in both cases the crystallization temperature is increased by about 13 °C.

Similar conclusions on plasticization and crystallization behaviour can be obtained from the velocity curves. Ultrasonic velocity in the solid state is known to increase with the presence of fillers [19,20], as generally the solid particles increase the elastic modulus more rapidly than the density. In the melt, the situation is more complex and scattering phenomena have to be taken into account. The velocity in that case can decrease or increase depending on the size, the number and the modulus of the particle. Talc in small concentration usually increases the velocity, although this effect is barely visible in Fig. 2(b). On the contrary, addition of CO_2 decreases the ultrasonic velocity as a consequence of plasticization, as it is clearly shown in Fig. 2(b).

3.2. Influence of temperature on degassing pressure

Typical evolutions with time of specific volume and attenuation when the applied pressure is modified are shown in Fig. 3 for a temperature set at 39 °C. In the first step, as the pressure is decreased, the attenuation slightly decreases until it starts to rise very rapidly due to the scattering of the ultrasound wave by the nuclei and the growing bubbles (Fig. 3(a)). The pressure associated to this break point corresponds to the said degassing pressure (see the dotted line in Fig. 3). As displayed on Fig. 3(b), the expanding cells also rapidly impact the specific volume curve, although this characteristic might also be sensitive to the significant dilation induced by the PBA near the equilibrium conditions. The pressure is thereafter maintained constant, i.e. as soon as nucleation and bubble growth occur. In the final step, increasing the applied pressure forced the dissolution of CO_2 back into the PCL matrix. At the end of the sequence, it is interesting to note that the specific volume is

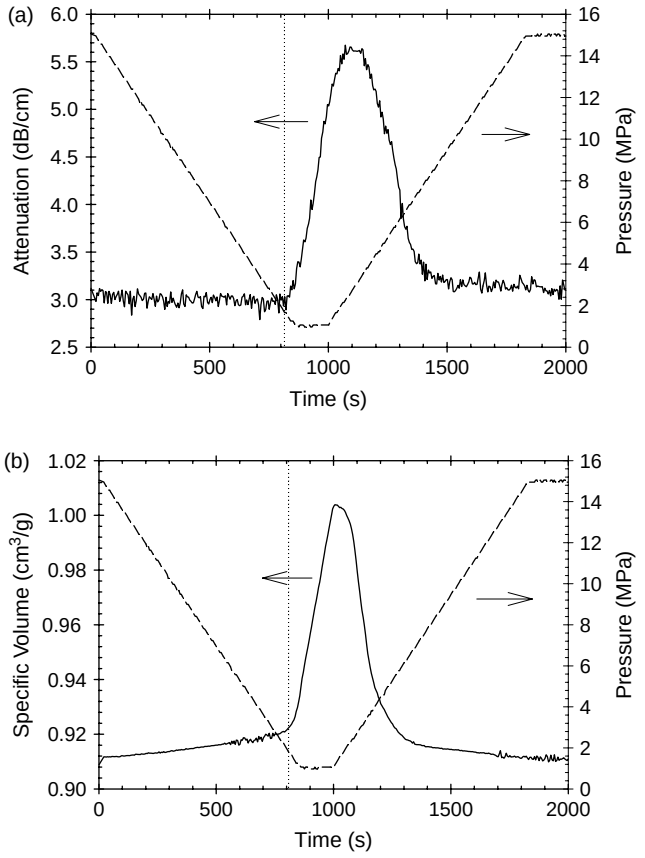

Fig. 3. Evolution of (a) attenuation, (b) specific volume and (a and b) pressure during typical degassing experiments for PCL/5 wt% talc/5 wt% CO_2 at $T=$ 39 °C. The vertical dotted line shows the time corresponding to the degassing onset and is given only as a guide for the eyes.

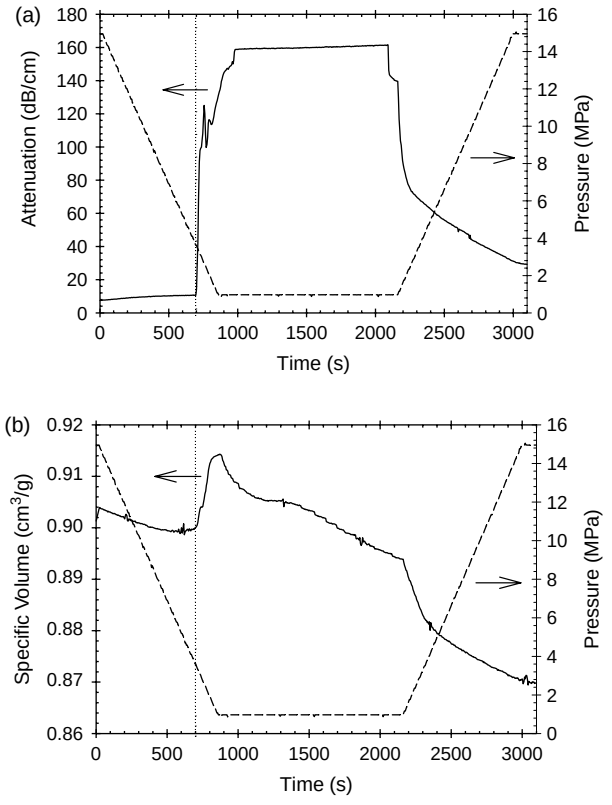

Fig. 4. Evolution of (a) attenuation, (b) specific volume and (a and b) pressure during typical degassing experiments for PCL/5 wt% talc/5 wt% CO_2 at $T=$ 34 °C. The vertical dotted line shows the time corresponding to the degassing onset and is given only as a guide for the eyes.

exactly the same as that observed at the beginning of the degassing experiment. This behaviour, also observed at other higher temperatures, is characteristic of a completely amorphous sample. However, measurements of the degassing conditions of the same sample but investigated at a lower temperature ($T=34$ °C) and reported in Fig. 4 illustrate a completely different specific volume evolution. It can clearly be seen that the specific volume measured at the end of the experiment (beyond time of about 3000 s; $P=15$ MPa) is far lower than that obtained at the beginning of the pressure ramp ($\Delta V_{sp} \cong 0.034$ cm^3/g), thus indicating that crystallization occurred. More interestingly, it can be unambiguously demonstrated from the decrease of specific volume at early times ($t<600$ s) that crystallization starts before the nucleation and growth of gas bubbles. The degassing pressure estimated through this experiment gives a high value of 3.6 MPa.

It is also worth noting that the variation in specific volume associated with foaming of the crystalline sample ($\Delta V_{sp} <$ 0.02 cm^3/g) is rather small compared to the expansion observed for completely amorphous sample ($\Delta V_{sp} > 0.08$ cm^3/g) and this effect cannot be only attributed to the foaming temperature ($\Delta T \cong 5$ °C). It is recognized that the presence of crystals has a drastic effect on the viscoelastic behaviour of the polymer/PBA solution. For instance, Baldwin et al. [7] demonstrated that the storage modulus of crystalline PET/CO_2 mixture can be enhanced by a factor up to ten, compared to that of a mixture with amorphous PET, for the same gas concentrations. Thus, in comparison to the amorphous phase, the cell growth mechanism of semi-crystalline foam is not governed only by the diffusion process, but also by the viscoelastic behaviour of the polymer/gas solution. As a result, this higher matrix stiffness reduces the expansion of the foam. On the other side, the attenuation signal raised well above 100 dB/cm for the crystalline sample, compared to less than 10 dB/cm for the full amorphous sample foamed at 39 °C for equivalent foaming time. To our opinion, this behaviour may be explained by a very high nucleation density of bubbles and/or by the presence of an open-cell structure, according to the morphology reported in our previous work [13] and mentioned earlier in the introduction part (Fig. 1).

To summarize all the above results, Fig. 5 shows the variation of the degassing pressure as a function of temperature for the neat PCL and PCL/5 wt% talc samples containing 5 wt% of CO_2 in both cases, where each point corresponds to a specific degassing experiment conducted at a given temperature. From these data, one can note several important facts:

(i) For 100% amorphous state ($T>40$ °C), increasing the temperature moderately increases the degassing pressure in a linear fashion. In quasi-static conditions (i.e. without any shear field as those encountered under flow conditions such as in extrusion processing), it is

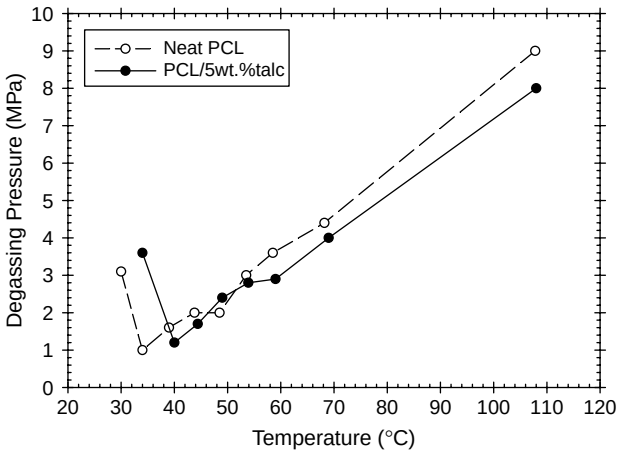

Fig. 5. Evolution of the degassing pressure determined from the attenuation curves pressure as a function of temperature. In both cases, the CO_2 concentration is set to 5 wt%.

generally accepted to link the ultrasonic measurements to the solubility of the physical blowing agent within the polymer. Since, the PBA concentration into the sample is kept constant at 5 wt% during all the investigation procedure, the increase of degassing pressure with temperature simply depicts the lower solubility of CO_2 in PCL at higher temperatures.

(ii) Another interesting feature related to this linear trend concerns the effect of talc on the degassing pressure. As shown in Fig. 5, the degassing pressures determined for the neat PCL and PCL/5 wt% talc samples fall within a rather narrow band not much wider than the experimental error, estimated as ± 0.5 MPa. Thus, it can be concluded that there is no significant effect of the talc on the degassing pressure in the amorphous phase. This result is quite surprising since it has been reported elsewhere using the same ultrasonic technique [5] that the presence of a nucleating agent such as talc shifted to a higher level the degassing pressure by as much as 1.2 MPa, with this effect prevailing over a wide range of temperature. However, these observations were made during extrusion, i.e. in presence of flow conditions and shear fields, compared to our measurements performed on a confined, static sample. On the other side, it was shown in our previous work [13] that increasing the talc content from 0.5 to 5 wt% increased the cell nucleation density as well as it improved the foam quality. At the present time there is no clear explanation why the presence of talc particles did not lead in the present case to an increase in the degassing pressure as expected, whereas it seems to clearly improve the cell nucleation with respect to the final product.

(iii) The most striking feature in Fig. 5 is the abrupt 3 to 4-fold increase in degassing pressure for temperatures below 40 °C, i.e. in the presence of a crystalline phase. As shown in Fig. 4 for the PCL/5 wt% talc/CO_2 system, the decrease in specific volume observed during the decompression experiment indicates that crystallization is taking place, which strongly suggests that crystal formation enhances nucleation. In addition, it is interesting to note that this abrupt increase in degassing pressure occurs at a higher temperature in the presence of talc. Obviously, this is due to the role that talc particles played as nucleating agent for the crystal formation, which shifted crystallization at a higher temperature. The influence of talc content on the crystallization temperature was clearly demonstrated in our previous study using DSC measurements [13] as well as in Section 3.1 (non-foaming experiments, temperature sweeps) with or without CO_2. Thus, these results can be coupled to our previous work [13] in which it has been observed that the cell population density of the PCL/5 wt% talc sample changes dramatically below a foaming temperature of 35 °C. More precisely, the cell density at a foaming temperature of 28 °C is 1000-fold higher than that obtained for the sample foamed at 35 °C. In principle, a higher cell population density originates from the presence of a higher number of nucleation sites. This strongly suggests that crystal formation enhances nucleation. As mentioned in the introduction part, similar results have been published in the literature for other polymer/PBA systems but, to our knowledge, this is the first report of the influence of crystal formation on the pressure conditions for phase separation.

3.3. Influence of crystalline fraction on degassing pressure

In order to thoroughly investigate the influence of crystal formation on degassing pressures, additional samples were submitted to successive degassing experiments conducted in isothermal conditions. The choice of the suitable isothermal temperature was dictated for both samples (with or without talc) by two major factors: on one side, this temperature must be low enough to ensure crystallization of the samples. But on the other side, the crystallization rate at that temperature must be slow enough to allow the measurement of several degassing pressures before the completion of the crystallization event. We also have to keep in mind that presence of talc increases the crystallization temperature and therefore it was not possible to use the same temperature for both samples (with and without talc). Fig. 6 shows the evolution of specific volume and pressure as a function of time for a PCL/8.2 wt% CO_2 sample and a temperature of 30 °C. The evolution of specific volume is plotted against time starting from the moment when the sample reaches the desired temperature of crystallization. The change in crystalline fraction throughout the degassing experiments was assessed by using the evolution of the specific volume as a function of time at the same temperature but without any pressure ramp, with the pressure being kept constant at 10 MPa, and by assuming that the effect of the several pressure ramps and the corresponding induced foaming periods on

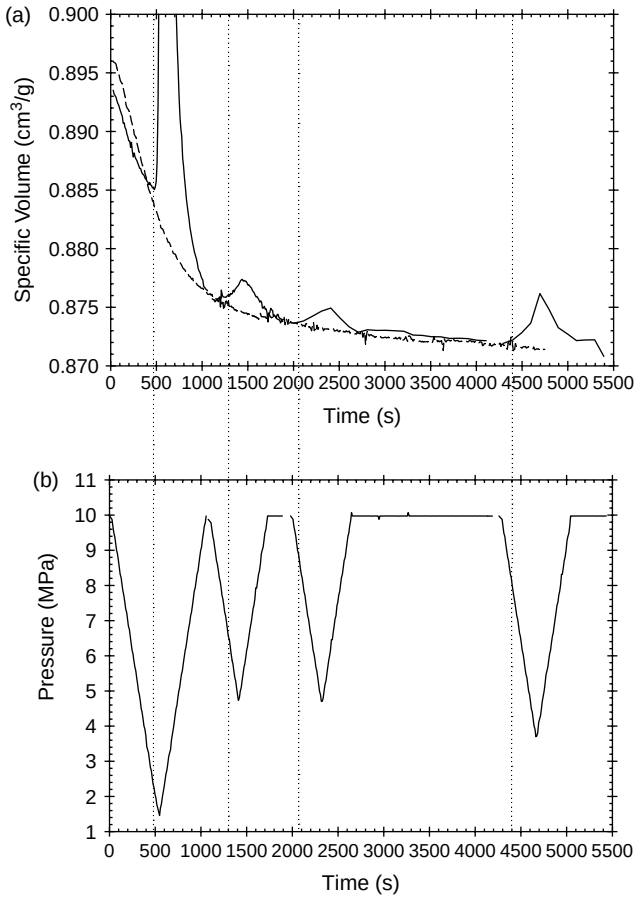

Fig. 6. Evolution of (a) specific volume as a function of time as (b) the applied pressure was changed for PCL + 8.2% CO_2 sample and a temperature of 30 °C. The evolution of specific volume as a function of time at the same temperature but without pressure ramp is also reported here (dashed line). This curve is used both to estimate the crystalline fraction corresponding to each degassing experiment and to demonstrate that the crystallization event is not significantly influenced by the pressure ramps.

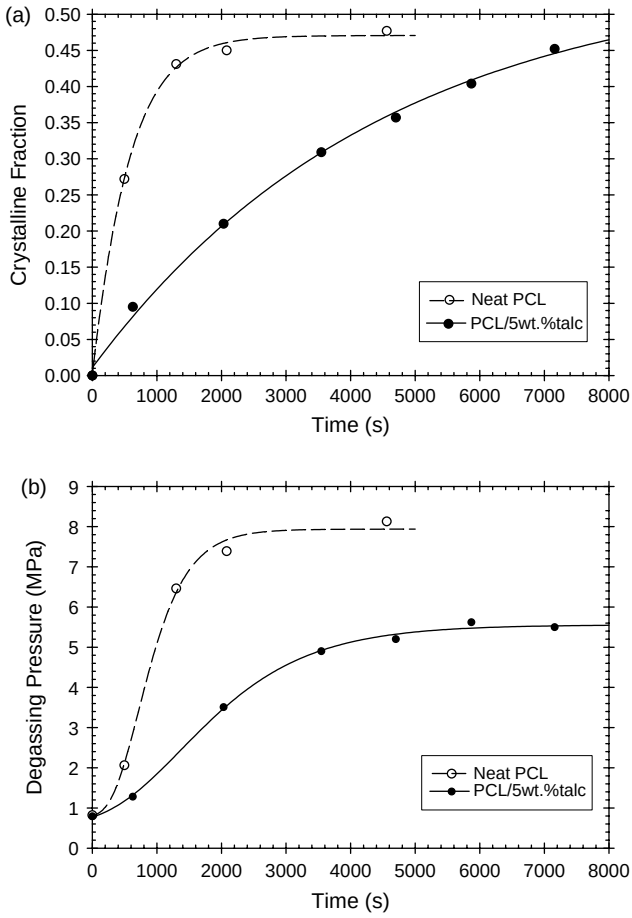

Fig. 7. Evolution of (a) crystalline fraction and (b) degassing pressure fraction as a function of time for neat PCL and PCL/5 wt% talc samples. The isothermal temperature was set to 30 and 39.5 °C for the neat PCL and PCL/talc samples, respectively. Note that the concentration of CO_2 estimated at the end of the experiment are 8.2 and 4.5 wt% for the neat PCL and PCL/talc samples, respectively. Note that the degassing pressures for completely amorphous samples were extrapolated from degassing experiments at higher temperatures.

crystallinity was negligible. Obviously, this last hypothesis is validated by the quasi superposition of this curve (dashed line) with the specific volume monitored during the successive degassing experiments, as shown in Fig. 6(a). The very weak variation (with time) of the specific volume at the end of the overall experiment indicates that the crystallization event was almost completed. It was assumed in first approximation that the crystalline fraction at the plateau value of the specific volume was close to 0.5. This value corresponds to an upper value since the crystalline fraction should slightly decrease with increased CO_2 concentration, as mentioned in our previous work using high pressure DSC [13]. For both sets of data, the overall decrease of the specific volume was approximately 0.021 cm^3/g, indicating a similar level of crystallinity at the end of each sequence.

The resulting crystalline fractions and their corresponding degassing pressures are reported in Fig. 7 for neat PCL and PCL/talc samples. In addition, to better understand the role played by crystallinity on degassing pressure, it is helpful to report differently the data of Fig. 7 by plotting the evolution of degassing pressure as a function of the crystalline fraction, as shown in Fig. 8. One should note that the temperatures and CO_2 contents are slightly different between these two sets of data, respectively, 30 °C and 8.2 wt% CO_2 for the neat PCL and 39.5 °C and 4.5 wt% for the PCL/talc sample. It is also worth noting that the degassing pressures for completely amorphous samples were extrapolated from degassing experiments done at higher temperatures. Despite different isothermal temperatures and CO_2 gas concentrations, the degassing pressures in completely amorphous samples are almost the same within the experimental error, thus simply indicating that the higher concentration of CO_2 compensates adequately for the lower temperature.

At this point of the discussion, it is interesting to compare the degassing pressure of the completely amorphous sample with equilibrium solubility data. Fig. 9 depicts the equilibrium solubility of CO_2 (see Ref. [13] for details about the experimental part) in neat PCL and PCL/5 wt% talc samples as a function of saturation pressures, as measured at room temperature. In both cases, the crystalline fraction measured by DSC before saturation with CO_2 was 50 wt% and did not change during saturation. The amount of gas uptake of CO_2

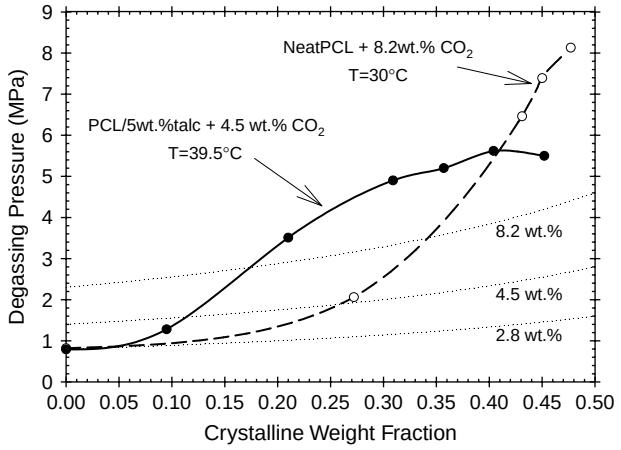

Fig. 8. Evolution of degassing pressure as a function of crystallinity for neat PCL and PCL/5 wt% talc samples. The isothermal temperature was set to 30 and 39.5 °C for the neat PCL and PCL/talc samples, respectively. Note that the concentrations of CO_2 estimated at the end of the experiment are 8.2 and 4.5 wt% for the neat PCL and PCL/talc samples, respectively. The dotted lines represent the pressure required to dissolve a given amount of CO_2 in the amorphous phase. See Section 3.3 (i) for details about the pressure estimation procedure. Note that the degassing pressures for completely amorphous samples were extrapolated from degassing experiments at higher temperatures.

(expressed in grams of CO_2 per gram of polymer) remains almost linear up to a pressure of approximately 4.1 MPa. The equilibrium solubility for a completely amorphous sample, estimated from the 50% crystalline samples, are also reported in Fig. 9 (dotted line). Thus, the required pressure to dissolve 8.2 wt% of CO_2 at room temperature is around 2.3 MPa, which is far higher than the 0.8 MPa degassing pressure reported for the neat PCL sample as shown in Fig. 8 at almost the same temperature (30 °C). Quite surprisingly at first, this result may be explained as follows. Even though the measurement of degassing pressure may be an effective means of comparing the solubility behavior of different blowing agents, it does not

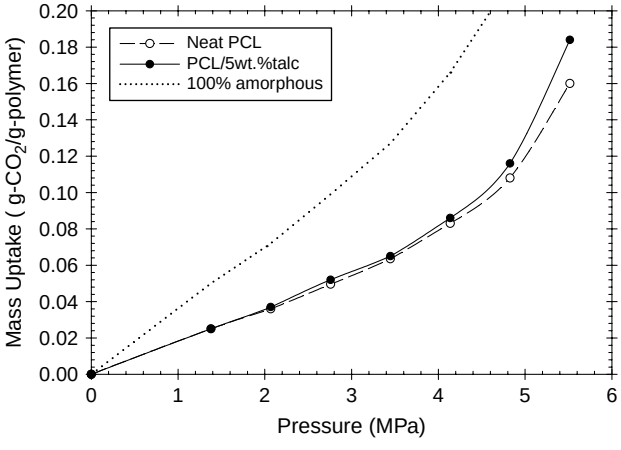

Fig. 9. Evolution of the equilibrium solubility of CO_2 in neat PCL and PCL/5 wt% talc samples as a function of saturation pressures measured at room temperature. In both cases, the crystalline fraction measured by DSC before saturation with CO_2 was 50 wt% and did not change significantly during saturation. The equilibrium solubility for a completely amorphous sample, estimated using Eq. (1) from the 50% crystalline sample results, is also reported as a dotted line.

necessarily corresponds to the equilibrium solubility. In some cases, the viscoelastic response of the polymer/PFA mixture to shear/elongational flow, i.e. during the foam extrusion process, may result in a degassing pressure much higher than that expected from solubility data [6]. On the other side, it has been found under static conditions (no flow) and with low-diffusivity blowing agents (HFC-134a in PS for instance) that the degassing pressures were much lower than the solubility equilibrium pressures [21]. In other words, that means that the onset of phase separation does not occur necessarily at the bimodal curve, which corresponds to the equilibrium solubility. The system may undergo supersaturation at a lower pressure, i.e. in the metastable region, before experiencing phase separation. To illustrate this point, PCL/talc samples charged with CO_2 were submitted to various decompression levels varying between 4.8 and 0 MPa by step of around 0.69 MPa. Fig. 10 shows the sample morphology obtained for the various decompression levels (P_{decomp}) investigated. The white traces in Fig. 10, barely visible but still noticeable, are the talc particles, which have a average size of 2 μm. It can clearly be seen that the bubble formation starts below 2.07 MPa, which is well below the equilibrium solubility pressure of 5.1 MPa corresponding to a temperature of 32 °C [13]. That yields a pressure difference (ΔP) of 2.4 MPa, this value being an indication of how far away the material is from the bimodal/solubility equilibrium line. Such high value of ΔP may indicate that the nucleation of bubbles is thermodynamically difficult to induce, even with the addition of talc. It is generally expected that the presence of a nucleating agent such as talc would trigger the nucleation by decreasing the amplitude of the free energy barrier and accordingly would reduce significantly the value of ΔP. From the results displayed in Fig. 5, a nucleating agent such as talc does not seem to increase the degassing pressures, thus indicating that talc may not be a very efficient nucleating agent for PCL/CO_2 system.

Going back to Fig. 8, for the sample with talc, as the crystallinity fraction increases, the degassing pressure moves upward slowly up to a point corresponding to a crystalline fraction near 10 wt%, where it then rises abruptly and eventually reaches a plateau. For the neat PCL, this abrupt change occurs at a higher crystalline fraction, roughly 30 wt%. One can observe that this point significantly differs from one type of sample to the other, despite the same degassing pressure observed for the completely amorphous samples. The most striking fact of this plot is the 6 to 10-fold increase in degassing pressures associated with the presence of crystallites, with respect to completely amorphous samples. In the next sections of this paper, different possible physical mechanisms will be envisaged in order to explain the above results.

3.3.1. Gas molecules expelled from crystallites

First consider the effect of crystal formation on the concentration of PBA. Since, it is well accepted that the gas molecules are expelled out from the crystal into the amorphous phase during crystallization, an argument based on the increase in gas concentration in the amorphous phase could be used as a potential explanation of the increase in degassing pressure

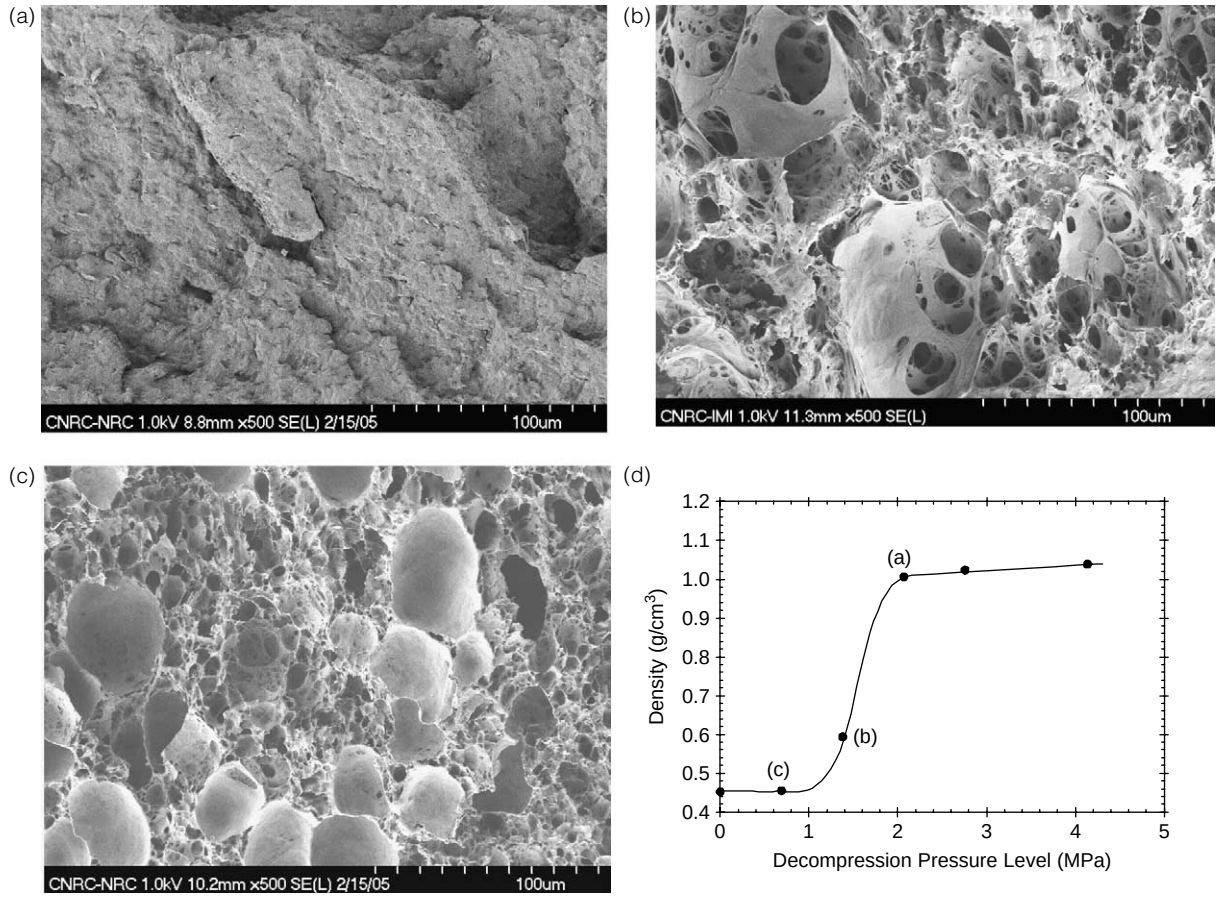

Fig. 10. Evolution of the morphology PCL/5 wt% talc samples as a function of decompression levels at a temperature of 32 °C. (a) $P_{decomp}=2.07$ MPa; (b) $P_{decomp}=1.37$ MPa; (c) $P_{decomp}=0.69$ MPa. Note that the cellular morphology obtained for the decompression pressure corresponding to ambient pressure is the one reported in Fig. 1. In all cases the PCL//talc samples were saturated with CO_2 for 3 h at 70 °C and a CO_2 pressure of approximately 6.2 MPa. (d) Influence of decompression pressure level on the density of PCL/5 wt% talc samples at a foaming temperature of 32 °C. The letters in parenthesis correspond to the morphology of the sample depicted above. The line is only a guide for the eyes.

assessed by ultrasonic measurements. In our experimental setting, the concentration of PBA into the overall sample is constant because the sample is confined into the chamber. As a consequence, the equilibrium mass uptake of the gas into the amorphous part of a semi-crystalline polymer must be corrected with respect to the fraction of crystalline phase as expressed by

$$M_a = \frac{M_{sc}}{(1-\chi_c)} \quad (1)$$

where χ_c is the crystalline weight fraction, M_{sc} and M_a the mass uptake (wt%) of CO_2 in the overall semi-crystalline sample and only into the amorphous phase, respectively. This implies that the crystallization process should result in an increase of the concentration of CO_2 into the amorphous phase, and thus corresponding higher degassing pressures should be obtained. For an estimation of this theoretical increase in degassing pressure with crystallinity, it is worth comparing the measurements of the degassing pressure with the equilibrium solubility of CO_2 gas at different gas pressures. As mentioned in Section 3.3, the dotted line in Fig. 9 depicts the equilibrium solubility of completely amorphous sample as a function of the saturation pressure measured at room temperature. This latter curve is used to estimate the required pressure to dissolve 2.8, 4.5 and 8.2 wt% CO_2 as reported on the *y*-axis of Fig. 8 and which corresponds to the origin ($\chi_c=0$) of the dotted lines. Effect of temperature on the solubility was neglected. The estimated required pressure for semicrystalline samples (dotted lines) are estimated using Eq. (1), assuming constant overall carbon dioxide concentration, which implies increasing CO_2 content in the amorphous phase. Accordingly, the degassing pressure evolution depicted in Fig. 8 should increase proportionally to the crystalline fraction (see dotted line), according to Eq. (1). This is clearly not the case, except at low crystalline fraction, (typically lower than 10 wt%).

Surprisingly, the formation of crystals even in small quantity does not increase significantly the degassing pressure compared to its completely amorphous counterpart, which should be the case if crystals, even at a low crystalline content, play the role of nucleating agent for bubble nucleation through reduction of the energy gap. This indicates that homogeneous nucleation may still prevail in the system under investigation, despite the presence of the crystalline phase. According to Baldwin et al. [7], the mechanism underlying bubble

nucleation for a semi-crystalline polymer in presence of both amorphous and crystalline phases is the preferential formation of PBA critical clusters at the surface of crystal, thus decreasing the free energy barrier associated with the formation of stable nuclei and more importantly the number of potential nucleation sites. However, their samples with 5–10 wt% crystalline phase did not show any effect on cell nucleation density, whereas it should offer sufficient amorphous/crystalline interface to trigger cell nucleation. One also have to keep in mind that the formation of 'free' amorphous/crystalline interface—which are not constrained between adjacent crystallites or confined into pocket of occluded melt—decreases rapidly with crystalline fraction because of the impingement of spherulites. This latter point will be discuss in more details in the next case but it can already be claimed that it occurs at relatively low crystalline fraction.

3.3.2. Formation of PBA concentration gradient around crystallites

Next, consider the sudden increase in the degassing pressure well above the equilibrium solubility line that can be observed for crystalline fractions greater than 10 wt% for talc filled samples and greater than 30 wt% for neat PCL. We may attempt an explanation based on an increase of local gas molecule concentrations in the vicinity of the crystallite since the CO_2 molecules are expelled outside the crystallites. More precisely, some CO_2 molecules could be confined in the interlamellar amorphous region whereas the others should be rejected to the outside of the spherulite. Such kind of kinetic mechanisms have been well studied in polymer blends for the particular case of semicrystalline–amorphous systems with partial miscibility [22–25]. For instance, it has been shown for PCL/PS blends that crystallization of almost pure PCL spherulites can induce demixing. Large PS droplets are observed between the well-developed spherulites or on their surfaces [23] as a result of the higher concentration of PS at the surface of the crystallite growth front. According to these authors, the simultaneous occurrence of crystallization and phase separation was found to depend on the relative values of the growth rate v_c of the crystalline entities

$$v_c = \frac{dR}{dt} \tag{2}$$

where R is the radius of the spherulite, and the diffusion rate of the non-crystallizable molecules, v_d

$$v_d = \left(\frac{D}{\tau_c}\right)^{0.5} \tag{3}$$

where D represents the diffusion constant and τ_c a correction time [23] for the macromolecules, which both depend on the temperature. In the same manner, the phenomenon of crystallization in presence of a foaming agent can be approached in terms of phase separation. The concentration of PBA may be greater at the surface or around the crystallites, as compared to the concentration in the bulk amorphous phase, which may result in higher degassing pressures. In that sense, bubble nucleation may be triggered by crystallization, but it is worth noting that it is a completely different mechanism from classical heterogeneous nucleation, where the preferential nucleation of gas bubble is driven by surface energy reduction rather than kinetic considerations. If so, the presence of a concentration gradient should depend on the relation between the diffusion kinetics of the CO_2 gas molecules throughout the PCL amorphous phase, v_d, and the growth rate of the PCL crystal, v_c.

In spite of our poor knowledge of the crystallite growth rate in presence of CO_2 gas and of the diffusion coefficient of CO_2 into the PCL, one may attempt an estimation of the so-called Keith–Padden parameter ($\delta = D/v_c$) that represents the distance over which CO_2 gas molecules will be excluded from the growth front of PCL [25]. Small value of δ (typically in the order of μm) would indicate the presence of concentration gradients around spherulites. Based on results excerpted from our previous work [13], the diffusion coefficient for 50% crystalline PCL at 34 °C can be estimated as 5.2×10^{-7} cm^2/s. On the over hand, in the case of PCL, the growth rate of lamella can be computed from the work of Beekmans and Vancso [26], which gives a value of about 14×10^{-9} cm/s at 57 °C. So we can roughly estimate the δ ratio to be approximately 37 cm. Such huge value for the Keith–Padden parameter seems to indicate that the CO_2 molecules rejected from the crystallite could not possibly accumulate near the growth front of the spherulites. This result is not surprising since CO_2 molecules are relatively small and therefore can diffuse much quicker than polymer macromolecules.

However, one can still envisage non-homogeneity of the PBA concentration but at a larger scale level. This could be associated to the non-homogenous distribution of crystals in the matrix. This idea is well supported by observation of polarized micrographs obtained from different semicrystalline polymers such as PET, which clearly demonstrates that the distribution of spherulites at low crystalline fraction can be highly heterogeneous with high crystalline regions composed of numerous crystallites very close to each other compared to very poor crystalline regions of the same size but with very few crystallites or even free of crystals [9]. The preferentials localization of crystals around or at the surface of talc particles has been reported in the past, which may also potentially enhance the heterogeneity of the PBA concentration. Furthermore, since the gas molecules diffuse only through the amorphous phase, the presence of crystallites has the tendency to decrease the diffusivity of the PBA molecules by creating a more tortuous pathway for their displacement throughout the sample [27]. Therefore, the concentrations of the PBA around the highly crystalline regions may even be greater than those reported in the more amorphous regions. These concentration gradients, at a scale level of several crystallites, may be part of the explanation for the high degassing pressures reported in Fig. 8. As a result, the generation of regions with different PBA concentrations should result in the formation of a bimodal cell morphology: the high crystalline regions would result in a higher cell population density and smaller cell size because of the higher concentration of PBA and a very high stiffness due

to the presence of crystallites. On the contrary, the low crystalline regions would result in lower cell nucleation density but with higher cell size due to the lower PBA concentration and lower matrix stiffness. This explanation is strongly supported by the morphology of PCL/talc samples shown in Fig. 1 and discussed in our previous work [13].

3.3.3. Spontaneous formation of microvoids induced by crystallization

In another approach, it has been shown for two-dimensional samples (thin films) as well as in the three-dimensional case (bulk samples) that localized volume anomalies or singularities occur during the crystallization in liquid areas completely confined by spherulites [28–31]. Indeed, the impingement of spherulites in the course of crystallization leads to the formation of pockets of occluded polymer melt. On further crystallization, these occluded areas are the location of build–up of negative pressure (stress) because the melt is forced to move from the interior of the pocket toward the crystallization front and there is no supply of fresh melt to fill up the deficiency of material. These occluded areas can eventually result in localized volume defects through cavitation if the internal stress exceeds the limit of melt cohesion, or they simply can also remain frozen into the material. Nowacki et al. [30] nicely demonstrated from measurement of the growth rate of spherulites in isotactic polypropylene (iPP) films that stress build–up starts almost immediately after the moment of occlusion of the melt by the spherulites. It has been shown that the spherulite growth rate decreases continuously as the crystallization inside pocket of occluded melt proceeds. This occurs due to the build–up of negative pressure, which decreases the equilibrium melting temperature and hence reduces locally the undercooling. Galeski et al. [29] demonstrated for iPP that acoustic events associated with cavitation phenomena start close to the half-time of crystallization and that its maximum is close to the end of crystallization process ($\cong$95% completion). More importantly, it appears from their results that the formation of pockets of melt and hence the build–up of negative pressure starts at a time as low as one fourth of crystallization time. In our case, this corresponds to crystalline fractions around 10–15 wt%. This raises some questions on the effect of internal stress may have on the degassing conditions in the present work.

At this point of the discussion, it is interesting to go back to the work of Tatibouët and Gendron [6] on the influence of the flow conditions during extrusion foaming on the degassing pressures of polystyrene/HCFC–134a mixtures using an in-line detection method based on ultrasonic sensors. These authors quantitatively associated the increase of the apparent degassing pressure observed for the higher molecular weight resins with the higher first normal stress difference of the melt/PBA system generated during flow into the extruder. In particular, the anisotropy of stress level could reduce the local stress field in the flow direction, thus leading to higher apparent degassing pressure. In our case, one could also envisage that the generation of stress inside pockets of melt could facilitate the nucleation of gas bubble by decreasing the efficient pressure inside the pocket of melt compared to the hydrostatic pressure applied to the whole sample, and hence would result in higher apparent degassing pressure. Pawlak and Galeski [32] estimated that negative pressure values can reach the considerable value of 40 MPa for typical polymer melts! In our case, the stress level or negative pressure may be estimated by the difference between the measured degassing pressure and the degassing pressure only based on concentration effects into the amorphous phase (dotted line). A maximum value of 6.4 MPa was found for a crystalline fraction of 50 wt% for the PCL sample. The sudden increase in the degassing pressure corresponds relatively well with the estimated build–up of negative pressure ($X_c \cong 10$ wt%) for the PCL/talc sample. However, when looking at the evolution of degassing pressure with crystalline fraction for the PCL sample without talc, one can see that the breakpoint is shifted towards relatively high crystalline fraction, around 30–35 wt%, as compared to the PCL/talc sample. This discrepancy should be related to the presence of talc, which modifies the crystalline morphology.

Another interesting point concerns the degassing pressures obtained in the terminal region (higher crystalline fractions). According to Galeski et al. [29], the value of negative pressure inside pockets of occluded melt depends on the difference in density between melt and crystalline phase, the degree of conversion of melt into spherulites as well as the melt compressibility. In principle, this should not depend on the size of the 'weak' spots. However, in practice, the deformation of spherulites in the case of weak spots may significantly decrease the volume defect and hence decreases the magnitude of the negative pressure, eventually resulting in no cavitation. Talc is a good nucleating agent for the nucleation of PCL crystals, as demonstrated by the increase in crystallization temperature during cooling from the molten state (see section on unfoamed material). The presence of talc should result in spherulites of smaller sizes and thus to smaller melt pockets but in higher number. As a consequence, the maximum degassing pressure may be lower in the presence of talc, which seems to be the case in Fig. 8. The stress level inside melt pockets estimated at the end of the crystallization process is approximately 3.9 MPa for the PCL/talc sample, well under the value obtained for the neat PCL.

The results presented here strongly indicate that the formation of pockets of occluded melt, through the impingement of spherulites, may explain the abnormally high measured degassing pressures. However, it must be pointed out that this phenomenon should not trigger cell nucleation and growth in foaming process since these bubbles will be constrained into the impinged spherulites. Hence, the question of the origin of the finer morphology of semi-crystalline sample still remains. An argument based on the decrease of the molecular mobility of the polymeric chain due to the formation of crystals may potentially explain this phenomenon. In fact, it has been shown that the formation of crystalline regions do act as cross-links. These physical cross-links connect molecules into larger clusters, each of these clusters containing many crystalline domains. Similarly to what is observed for chemical crosslinking, a physical gel point (physical because it is

thermoreversible) is defined by the appearance of connectivity throughout the whole sample. Interestingly, it has been shown that liquid-to-solid transition (LST) strongly affects the molecular mobility, which as a result also leads to the dramatic change in rheological properties. The crystallinity at the gel point was found to vary upon the polymer with a relative crystallinity of around 6–15% for isotactic polypropylene [33] and around 20% for PCL sample [34]. According to Horst and Winter [35], the type of connectivity encountered during crystallization is provided by amorphous chains immobilized by segments attached to several crystalline structures. Obviously, this stage will precede the impingement of spherulites (formation of pocket of occluded melt). One could consider that the physical cross-links created at the early stage of crystallization may be enough to limit the growing of gas bubbles, thus leading to the enhancement of cell nucleation rate compared to completely amorphous sample. Furthermore, the crystallization process should not be considered as to be completely homogeneous. Rather, long-range heterogeneity of crystallization may exist within the sample if the crystallization process does not occur simultaneously throughout the sample. That phenomenon may lead to the bimodal cell structure observed in Fig. 1(b).

In summary, it appears from all the above that the increase in cell nucleation density generally observed in presence of crystalline phase cannot be attributed to heterogeneous contributions but rather to the high stiffness of the matrix, such as microcellular morphology is obtained without any cell nucleating agent.

4. Conclusion

A number of concluding remarks can be made from our investigation of the impact of crystallization on the foaming of PCL/CO_2 mixture using a batch process equipped with ultrasonic sensors.

It has been unambiguously demonstrated that the static ultrasonic measurement system is a powerful tool to determine whether the nucleation of crystallites precedes the formation of gas bubbles. In addition, different nucleation/growth mechanisms were distinguished through a careful analysis of the data: nucleation of gas bubbles for the amorphous sample is characterized by attenuation signal 10 times lower than in the crystalline sample, whereas the change in specific volume associated with the amorphous sample is several times greater compared to those observed for crystalline samples. These results should be compared to the foam morphology obtained on the same system in a previous work. Consequently, the formation of a high cell population density of small open cells is crystalline dependent. The most probable mechanism may be the reduction of molecular mobility of the polymeric chain, i.e. an increase in matrix stiffness, due to the formation of crystals that do act as crosslinking points.

The most striking result of our study is the huge increase in the degassing pressures observed for crystalline samples with respect to the amorphous system. Even if it strongly suggests that crystal formation enhances cell nucleation, the precise role of crystal on nucleation of gas bubble is not clear. On one side, this huge increase in degassing pressure cannot be solely attributed to blowing agent content or solubility issues. On the other side, heterogeneous nucleation would imply a huge increase in degassing pressure as soon as crystals appear, and that because of the lower energy barrier associated with the formation of a stable nuclei (bubble) onto the surface of the crystal, which seems not to be the case. Rather, the major increase in degassing pressure was associated with the build–up of negative pressure inside pocket of occluded melt, which typically begins in our case at a crystalline fraction of around 10–15%, for talc-induced crystallization.

Eventually, while talc particles are not very efficient in the amorphous phase to trigger the cell nucleation process—the degassing pressure for the sample with or without talc were almost the same their role in crystal nucleation at lower temperatures is obvious. Addition of talc shifts the crystal formation to higher temperature, and thus indubitably impacts the cell nucleation process.

References

[1] Colton JS, Suh NP. Polym Eng Sci 1987;27:485–92.
[2] Chen L, Wang X, Straff R, Blizard K. Polym Eng Sci 2002;42:1151–8.
[3] Areerat S, Hayata Y, Katsumoto R, Kegasawa T, Egami H, Ohshima M. J Appl Polym Sci 2002;86:282–8.
[4] Ramesh NS, Rasmussen DH, Campbell GA. Polym Eng Sci 1994;34:1685–97.
[5] Tatibouët J, Gendron R, Hamel A, Sahnoune A. J Cell Plast 2002;38:203–18.
[6] Tatibouët J, Gendron R. Proceedings of the society of plastics engineers annual technical conference, Chicago, USA; 2004. p. 2552–556.
[7] Baldwin DF, Shimbo M, Suh NP. J Eng Mater Technol 1995;117:65–74.
[8] Baldwin DF, Suh NP. In: Proceedings of the society of plastics engineers annual technical conference, Detroit, USA; 1992. p. 1503–7.
[9] Doroudiani S, Park CB, Kortschot MT. Polym Eng Sci 1996;36:2645–62.
[10] Handa YP, Zhang Z, Nawaby V, Tan J. Cell Polym 2001;20:241–53.
[11] Lin J, Shenogin S, Nazarenko S. Polymer 2002;43:4733–43.
[12] Mizoguchi K, Hirose T, Naito Y, Kamiya Y. Polymer 1987;28:1298–302.
[13] Reignier J, Gendron R, Champagne M. Proceedings of the society of plastics engineers FOAMS, Philadelphia, PA, USA; 2004.
[14] Tatibouët J, Piché L. Polymer 1991;32:3147–51.
[15] Piché L, Massines F, Hamel A, Néron C. US Patent 4754645, 1988.
[16] Sahnoune A, Tatibouët J, Gendron R, Hamel A, Piché L. J Cell Plast 2001;37:429–54.
[17] Liegey F, Tatibouët J, Derdouri A. Proceedings of the society of plastics engineers annual technical conference, Chicago, USA; 2004. p. 1300–304.
[18] Zhang Z, Nawaby AV, Day M. J Polym Sci, Part B: Polym Phys 2003;41:1518–25.
[19] Piché L. IEEE Ultrason Symp 1989;599–608.
[20] Gendron R, Tatibouët J, Guèvremont J, Dumoulin MM, Piché L. Polym Eng Sci 1995;35:79–91.
[21] Tatibouët J, Gendron R. Proceedings of the 7th International conference on blowing agent and foaming processes, RAPRA, Stuttgart: Germany; 2005.
[22] Jungnickel BJ. Lect Notes Phys 2003;606:208–37.
[23] Li Y, Stein M, Jungnickel BJ. Colloid Polym Sci 1991;269:772–80.
[24] Tanaka H, Nishi T. Phys Rev Lett 1985;55:1102–5.
[25] Tanaka H, Nishi T. Phys Rev A 1989;39:783–94.
[26] Beekmans LGM, Vancso GJ. Polymer 2000;41:8975–81.

[27] Vieth RW. Diffusion in and through polymers: principles and applications. Munich: Hanser Publishers; 1990.
[28] Galeski A, Piorkowska E. J Polym Sci, Part B: Polym Phys 1983;21: 1299–312.
[29] Galeski A, Piorkowska E, Koenczoel L, Baer E. J Polym Sci, Part B: Polym Phys 1990;28:1171–86.
[30] Nowacki R, Kolasinska J, Piorkowska E. J Appl Polym Sci 2001;79: 2439–48.
[31] Thomann R, Wang C, Fressler J, Mülhaupt R. Macromol Chem Phys 1996;197:1085–91.
[32] Pawlak A, Galeski A. J Polym Sci, Part B: Polym Phys 1990;28: 1813–21.
[33] Schwittey C, Mours M, Winter HH. Faraday Discuss 1995;101: 93–104.
[34] Acierno A, Di Maio E, Iannace S, Grizutti N. Rheol Acta 2005 [online].
[35] Horst RH, Winter HH. Macromolecules 2000;33:130–6.